

Effect of Surface Geometry on Adsorption and Desorption of Polymer Chains

Masami Kawaguchi* and Takaaki Arai

Department of Chemistry for Materials, Faculty of Engineering,
Mie University, 1515 Kamihama-cho, Tsu, Mie 514, Japan

Received April 11, 1990; Revised Manuscript Received August 13, 1990

ABSTRACT: Adsorption and desorption of polystyrenes (PS) at three different porous silica surfaces in cyclohexane have been performed in order to examine the effect of surface geometry on the adsorption and desorption phenomena of polymer chains as a function of the size ratio of the average pore diameter to twice the radius gyration of a PS chain. Dioxane was used as the displacer molecule. The adsorption isotherms for the porous silica surfaces are almost the same as for the nonporous silica in their shape. However, the plateau adsorbed amount increases with an increase in the size ratio. A similar surface geometry effect is also observed for the desorption of polystyrenes by dioxane. These phenomena can be interpreted in the terms of the surface fractal when the whole polymer chain is regarded as the yardsticks. The critical concentrations of the displacer molecule at which all PS chains can just be desorbed is almost independent of the pore size and the molecular weight of PS.

Introduction

Since the introduction of the concept of fractal geometry¹ reanalysis of the existing adsorption data has been extensively made by Avnir and co-workers.²⁻⁶ They deduced the simple accessibility scaling law between the interaction of adsorbates and surface, such as adsorbed amounts and molecular size. Of course, the surface geometry should have an effect on the polymer adsorption at the solid/liquid interface. Recently, Farin and Avnir⁶ have reanalyzed many adsorption studies, with special emphasis on polystyrene, and showed that a dense packing is formed by distorting the conformation of a polystyrene chain in the solution into a prolate shape on a flat surface and that the conformation changes only slightly upon adsorption on highly porous surfaces. Moreover, such general trends were found to be relatively insensitive to both the solvent power and the interaction between solvent and surface.

The displacement of polymer chains, in other words desorption of polymer chains from an adsorbent, has been achieved by increasing the concentration of a more strongly adsorbing solvent component, which is termed displacer molecule. At a certain critical concentration of the displacer molecules, the polymer chains are fully desorbed from the surface. This critical concentration is a clue to estimating the segmental adsorption energy in the terms of the theory of Cohen Stuart, et al.⁷ Some desorption experiments have been performed to estimate the segmental adsorption energy. As a result, reasonable values for the adsorption energy were obtained, which were very useful in understanding the polymer adsorption phenomena.⁷⁻¹⁰

The desorption process should also be controlled by the surface geometry, since it is considered as polymer adsorption from a binary solvent, which consists of solvent and displacer molecules. Equivalence of the desorption of preadsorbed polymer chains by the addition of the displacer molecules and the adsorption from the binary solvent at the same composition of displacer has been experimentally confirmed as far as both phenomena are concerned in the equilibrium state.¹¹ However, the effect of surface geometry on the desorption process of polymer chains is not well understood. The aim of this paper is to study both the adsorption and desorption phenomena of polystyrenes for well-defined porous silica particles as a

function of the size ratio of the average diameter of pore to twice the radius gyration of a polystyrene chain. The effect of the surface geometry on polymer adsorption and desorption will be discussed by comparison with those for the nonporous silica surface.

Experimental Section

Materials. Two polystyrene (PS) samples with narrow molecular weight distributions, having $M_w = 43.9 \times 10^3$ (PS-44) and 355×10^3 (PS-355) were purchased from Tosoh Co. The polydispersities of the PS-44 and PS-355 were determined to be 1.04 and 1.05, respectively, using a Toyo Soda HLC-802 A gel permeation chromatography instrument with a UV-8 Model II spectrometer. The wavelength used was 254 nm. The eluent solvent used was tetrahydrofuran.

Cyclohexane as a solvent and dioxane as a displacer and also a solvent for determination of PS concentration by UV spectroscopy were of spectroscopic quality, and they were used without further purification.

The silica particles used for the adsorbent were three porous microbead (100-200 mesh) silica gels (Fuji-David Chemical Co., Japan): MB-300 with the surface area (S) of 118 m²/g and an average pore diameter (d) of 28.5 nm; MB-800 with an S value of 45 m²/g and a d value of 81.3 nm; MB-1300 with an S value of 27 m²/g and a d value of 129.9 nm. The S values were determined by N₂ adsorption, and the d values were obtained from a mercury porosimeter. The latter method leads to the pore size distributions of the respective silicas as shown in Figure 1. From the detailed pore size distributions, we distilled two, D90 and D10, in addition to the mean, in order to more fully characterize the breadth and skewness of the distributions: 90% of the pore diameters are larger than the value of D90 and 10% are larger than the D10 value. For MB-300 D90 has the value 23 nm and D10 has the 44 nm; for MB-800 the values of D90 and D10 are 75 and 112 nm, respectively, while for MB-1300 they are 122 and 174 nm, respectively. The purified silica was obtained by washing with hot carbon tetrachloride with a Soxhlet apparatus for 3 days. The silica was dried in a desiccator under vacuum by using an aspirator and further dried in a vacuum oven at 130-150 °C for several days. These silica particles were kept in the vacuum oven to prevent contamination at room temperature before use.

Adsorption of PS. PS was dissolved in cyclohexane. A fixed amount of silica was transferred to a 50-mL flask to maintain a similar total surface area for the different silica particles (0.095 g for MB 300, 0.25 g for MB 800, and 0.415 g for MB 1300) and then mixed with 10 mL of cyclohexane. The sample in the glass flask was placed to allow the solvent to fully penetrate into the pores at 35 °C in an air incubator for 24 h. It was then mixed

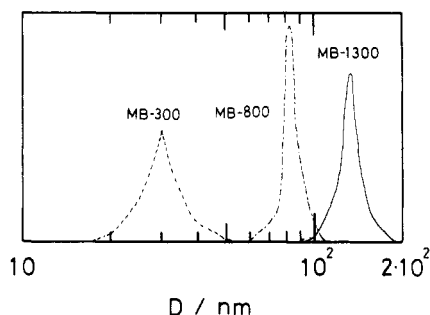


Figure 1. Pore size distributions of MB-300, MB-800, and MB-1300.

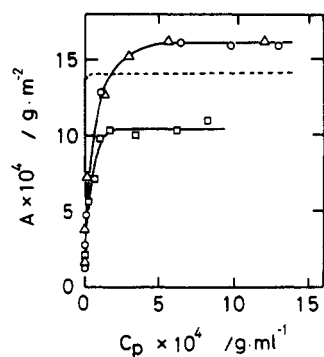


Figure 2. Adsorption isotherms of PS-44 for porous silicas in cyclohexane at 35 °C: (□) MB-300 with a size ratio of 2.5; (Δ) MB-800 with a size ratio of 7.0; (○) MB-1300 with a size ratio of 11.2. The dashed line indicates the adsorption isotherm of a PS with $M_w = 42.8 \times 10^3$ on the Aerosil 130 silica in cyclohexane at 35 °C.

with 10 mL of the cyclohexane PS solution. The mixture in the glass flask was mechanically shaken to attain equilibrium at 100 rpm in a Yamato BT-23 water incubator attached with a shaker for 24 h. The temperature of the water in the incubator was controlled to 35.0 ± 0.1 °C. After the silica particles were sedimented, the supernatant was carefully withdrawn. The PS concentration, C_p , in the supernatant was determined as follows: after the evaporation of the solvent, the residue was dried under vacuum and then dissolved in a known amount of dioxane by using an Ohstuka Denshi System 77 UV spectrometer to measure the C_p .

Desorption of PS. The procedure of the desorption of PS by dioxane in cyclohexane was performed by a method similar to that in the PS adsorption experiments described above. First, PS was dissolved in a binary mixture of cyclohexane and dioxane, and its PS solution was then mixed with the silicas soaked in the same binary solvent mixture. After this attained equilibrium, the PS concentration in the supernatant was determined by the same method as previously described. We selected the dosage concentration, $C_0 = 0.15$ g/100 mL, for every combination of PS and the silica.

To confirm the reproducibility of the experiments, we performed at least two measurements for the same concentrations. The error in the adsorbed amount was less than 5%.

Results and Discussion

Adsorption. Figure 2 shows the adsorption isotherms of the PS-44 onto the MB-300, MB-800, and MB-1300 silicas. The radius of gyration of the PS-44 sample in cyclohexane can be calculated to be 5.78 nm from the relation between the radius of gyration and the molecular weight.¹² Twice the radius of gyration of the PS-44 is smaller than the average pore sizes for all the porous silica surfaces. The size ratios of the average pore diameters to twice the radius of gyration of the PS-44 are 2.5, 7.0, and 11.2 for MB-300, MB-800, and MB-1300, respectively. Thus, it is considered that the PS-44 molecules can easily

penetrate into most of the pores without significant deformation of the PS chains. For comparison, the adsorption isotherm⁸ of a PS sample with $M_w = 42.8 \times 10^3$, on the nonporous Aerosil 130 silica is also displayed by the dashed line in the figure.

The adsorbed amount of PS, A , steeply increases at the lower concentrations and attains a plateau value. However, the initial slopes of the adsorption isotherms for the porous silicas are not as large as that of the adsorption isotherm for the nonporous silica. The plateau adsorbed amount depends on the pore size: the plateau adsorbed amount for the MB-800 silica is almost the same as that for MB-1300, is about 1.5 times as large as that for MB-300, and is larger than that for the nonporous silica. Similar pore size dependence of the adsorbed amounts was obtained by Furusawa et al.,¹³ but they made no attempt to interpret it.

According to the concept of the fractal geometry, the nonporous surface is regarded as a surface accessible for adsorption with the fractal dimension of 2.⁵ The fractal dimension of the Aerosil 130 was determined to be almost 2 by the adsorption experiments of nitrogen.⁴ However, analysis of the adsorption experiments of polystyrenes on the Aerosil 130 by plots of the number of PS molecules adsorbed per unit area from cyclohexane solutions as a function of the radius of gyration of PS in the cyclohexane solvent yields a fractal dimension of ca. 1.6.¹⁴ A similar fractal dimension was obtained for the other adsorption experiments of PS for the nonporous silicas, irrespective of the solvent power.⁶ On the other hand, the adsorption experiments of PS in cyclohexane on the porous Al_2O_3 surface in which PS chains can penetrate into their pores, gave ca. 2.9 for the fractal dimension of Al_2O_3 .⁶ The small fractal dimension of 1.6 is unreasonable because the fractal dimension of a surface accessible for adsorption should be larger than 2, and it should be discussed in the following paragraph.

A nitrogen molecule will see the nonporous silica as a smooth and flat surface with a dimension of 2 because the nitrogen molecular size is much smaller than the diameter of 16 nm with the Aerosil 130. In contrast with nitrogen gas, the diameters of PS chains in the solution are comparable to or larger than the dimensions of the silica particle, and the silica surface cannot be seen as the smooth flat surface from the perspective of the PS molecules. Moreover, although it is generally believed that the nonporous Aerosil particles are not aggregated themselves, which is confirmed by electron microscope observation,^{4,15} this situation should be changed by dispersing them in a solvent or by mixing them with polymer solutions. In a solvent such as water and organic solvents, the nonporous Aerosil silica tended to make a small aggregate.^{16,17} When the Aerosil silicas are mixed with a polymer solution, polymer adsorption follows aggregation of the silicas: a silica aggregate produced in solvent will behave as a kind of a knot or cross-linked point for polymer chains, that is, a polymer chain adsorbs across the surfaces of several silica particles, and this induces the silica aggregates to approach each another and finally leads to the flocculation of the silica particles by adsorbed polymer chains. In fact, the added PS chains in some adsorption experiments have induced the flocculation of the Aerosil silica.^{8,18} Thus, the resulting flocculated nonporous Aerosil 130 silica can be regarded as a kind of porous media, and its structure should resemble to the porous silica.

When we discuss the surface geometry effect on the adsorption experiments, the dimensions of polymer chains should be an important factor. Therefore, we would like

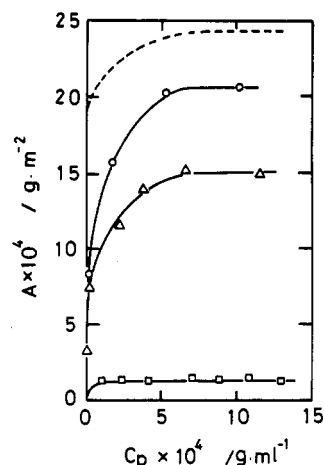


Figure 3. Adsorption isotherms of PS-355 for porous silicas in cyclohexane at 35 °C: (□) MB-300 with a size ratio of 0.9; (Δ) MB-800 with a size ratio of 2.5; (○) MB-1300 with a size ratio of 4.0. The dashed line indicates the adsorption isotherm of a PS with $M_w = 422 \times 10^3$ on the Aerosil 130 silica in cyclohexane at 35 °C.

to interpret the difference in the adsorbed amounts for the porous silicas from the viewpoint of regarding the whole polymer as the yardsticks. Although the porous silicas have somewhat wide pore size distributions as shown in Figure 1 in comparison to the polymer radius of gyration, it seems that there are no fractions that are quite small. Thus, all pores should be available for adsorption of PS-44. The large difference in the plateau adsorbed amounts for MB-300 and MB-800 arises from the PS-44 molecules being unable to see the same fractal surface for both silicas. The size ratio for the MB-800–PS-44 pair is about 3 times larger than that for the MB-300–PS-44 pair. Thus, for the PS-44, the pores in MB-300 should be seen as a fractal surface with the fractal dimension higher than those in MB-800. In other words, the surface geometry of MB-300 is more complex than that of MB-800. Similar results were obtained by computer simulation experiments of the adsorption of circular molecules on the fractal curves with a constant contour length as a function of radius,¹⁹ which showed that the number of circular molecules required to reach a full monolayer coverage decreases with an increase in the fractal dimension. On the other hand, regardless of the larger size ratio for the MB-1300–PS-44 pair than that for the MB-800–PS-44 pair, both adsorption isotherms are quite similar. This may indicate that the PS-44 chains cannot distinguish between MB-800 and MB-1300 in terms of the fractal dimension.

Figure 3 shows the adsorption isotherms of the PS-355 on the MB-300, MB-800, and MB-1300 silica surfaces. For comparison, the adsorption isotherm⁸ of a PS sample with $M_w = 422 \times 10^3$ for the nonporous Aerosil silica is shown in the figure. Twice the radius of gyration of PS-355 can be calculated to be 32.8 nm in cyclohexane, and it is larger than the pore size in MB-300 but smaller than that in MB-800 and MB-1300. From the diameters of the pores and PS-355, the size ratios obtained are 0.9, 2.5, and 4.0 for MB-300, MB-800, and MB-1300, respectively. From the pore size distribution of MB-300, ca. 20% of the pores are larger than the diameter of PS-355, and the effective surface area available for the adsorption of PS-355 should be reduced. As expected, the plateau adsorbed amount for MB-300 is much less than that of PS-44 for MB-300.

In contrast with MB-300, the PS-355 molecule can be easily enter the pores in MB-800 and MB-1300. The adsorption isotherms for MB-800 and MB-1300 are similar to those for the adsorption of PS-44 onto MB-300, MB-

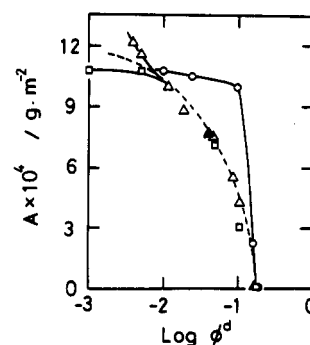


Figure 4. Desorption isotherms of PS-44 for porous silicas in a solvent mixture of cyclohexane and dioxane at 35 °C. The symbols are the same as in Figure 2. The filled triangle corresponds to a data point obtained from the desorption experiment of the preadsorbed PS-44 from MB-800 by adding dioxane. The dashed line indicates the desorption isotherm of a PS with $M_w = 42.8 \times 10^3$ for the Aerosil 130 silica in a solvent mixture at 35 °C.

800, and MB-1300 in their shapes. The plateau adsorbed amounts increase with an increase in the size ratio, and they are much larger than that for MB-300. From the pore size distributions of both silicas, most of the pores in them are available for the adsorption of PS-355. The difference in the plateau adsorbed amounts stems from the fact that the geometry in the pores for MB-800 is more complex than that for MB-1300 from the perspective of PS-355.

Desorption. Figure 4 shows the desorption isotherms of PS-44 for the MB-300, MB-800, and MB-1300 silicas, i.e., a plot of the adsorbed amount of PS-44 from the binary mixture of dioxane and cyclohexane versus the logarithm of the volume fraction of dioxane, ϕ^d , in the mixture. For comparison, the desorption isotherm⁸ of a PS sample with $M_w = 42.8 \times 10^3$ for the nonporous Aerosil 130 silica surface is also displayed in Figure 4.

As seen from Figure 4, the two desorption isotherms for MB-300 and MB-800 are similar to that for the Aerosil silica in their shapes for $\log \phi^d > -2$: the adsorbed amount rather steeply decreases with increasing $\log \phi^d$ and eventually becomes zero at a given ϕ^d , which we hereafter call the critical displacer concentration and designate ϕ_{cr}^d . The value of ϕ_{cr}^d is almost independent of the type of the silica used and is in good agreement with that for the nonporous silica surface.⁸ However, close inspection shows that the adsorbed amount for MB-800 is slightly larger than that for MB-300 at the same concentrations of dioxane. However, for $\log \phi^d < -2$ the divergence in the adsorbed amounts between MB-300 and MB-800 is enhanced as ϕ^d approaches zero. On the other hand, for the desorption experiment for MB-1300, the adsorbed amount becomes zero with a steeper slope and the adsorbed amount at a high concentration of dioxane, $\log \phi^d \sim -1$, is clearly larger than those for MB-300 and MB-800.

While in the case of adsorption isotherms the largest difference is between the MB-300 and MB-800 data, in the case of desorption isotherms the largest difference is between the MB-800 and MB-1300 data. This dissimilarity may mainly result from the fact that the dimensions of PS-44 in mixed solvents of cyclohexane and dioxane, which correspond to a good solvent for PS chains, are larger than for those in cyclohexane. This difference would mean a smaller size ratio for the desorption experiment. However, it still seems possible that the desorption process is also strongly affected by the surface geometry, similar to that for the adsorption behavior.

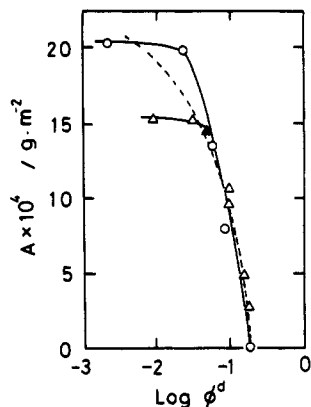


Figure 5. Desorption isotherms of PS-355 for porous silicas in a solvent mixture of cyclohexane and dioxane at 35 °C. The symbols are the same as in Figure 3. The filled triangle corresponds to a data point obtained from the desorption experiment of the preadsorbed PS-355 from the MB-800 by adding dioxane. The dashed line indicates the desorption isotherm of a PS with $M_w = 422 \times 10^3$ for the Aerosil 130 silica in a solvent mixture at 35 °C.

In Figure 5, the desorption isotherms of PS-355 from MB-800 and MB-1300 by dioxane are displayed. Changes in the concentrations before and after adsorption for high dioxane concentrations are smaller than those for MB-800 and MB-1300, and errors of the adsorbed amounts exceed 15%. Thus, the desorption isotherm of PS-355 is not shown in the figure. For comparison, the desorption isotherms of a PS sample with $M_w = 422 \times 10^3$ for the nonporous Aerosil 130 silica⁸ is also plotted. Two desorption isotherms for the MB-800 and MB-1300 silicas are similar in their shapes, and they are almost in agreement with that for the nonporous silica for $\log \phi^d > -1.5$. In contrast, for $\log \phi^d < -1.5$ the desorption isotherm curves show an obvious dissimilarity in their shapes, and they deviate from the curve for nonporous silica. The reason the desorption isotherm for the nonporous silica crosses the isotherms for the porous silicas is not clear, but it is noticed that the adsorbed amounts for the porous silicas for $\log \phi^d < -1.5$ are almost equal to the plateau adsorbed amounts for the adsorption isotherms in cyclohexane.

The values of ϕ_{cr}^d are almost the same, and their magnitude is coincident with that for the small PS-44 molecules. Independence of the ϕ_{cr}^d value from the PS molecular weight for both the nonporous⁸ and porous silica surfaces is reasonably interpreted by recalling that the critical concentration of the displacer molecules correlates with the difference in adsorption energy between a polymer repeating unit and a solvent molecule as required by the theory of Cohen Stuart et al.⁷ when similar chemical adsorbents are used.

The filled triangles in Figures 4 and 5 indicate the data points, which were obtained from the desorption ex-

periments of preadsorbed PS molecules by adding dioxane. Both points are well fitted on the respective displacement isotherm curves. From this agreement, we believe that the adsorption from a binary mixture is equivalent with the desorption of preadsorbed polymers. Similar behavior was observed for the displacement of PS chains from the nonporous silica surface.¹¹ However, kinetics for both processes are very different.²⁰ The adsorption of PS from a binary mixture took over several hours to reach equilibrium, while the desorption was sufficiently rapid to attain equilibrium within 1 h.

Conclusions

The surface geometry of the adsorbent surface strongly affects the adsorption and desorption processes. The adsorption isotherm for the porous silicas shows a somewhat rounded shape and is different from the high-affinity type, which is typical for polymer adsorption on a nonporous silica surface. The difference in the shapes of their adsorption isotherms and the plateau adsorbed amounts among the porous silicas result from the size ratio of the pore diameter to polymer dimensions. The larger size ratio corresponds to a less complex geometry, namely, the smaller fractal dimension in the pores from the perspective of the whole polymer chain. This concept can be useful for an interpretation of polymer desorption behavior.

References and Notes

- (1) Mandelbrot, B. B. *The Fractal Geometry of Nature*; Freeman: San Francisco, 1982.
- (2) Avnir, D.; Pfeifer, P. *Nouv. J. Chim.* **1983**, *7*, 71.
- (3) Pfeifer, P.; Avnir, D. *J. Chem. Phys.* **1983**, *79*, 3558.
- (4) Avnir, D.; Farin, D.; Pfeifer, P. *J. Chem. Phys.* **1983**, *79*, 3566.
- (5) Avnir, D.; Farin, D.; Pfeifer, P. *Nature* **1984**, *308*, 261.
- (6) Farin, D.; Avnir, D. *Colloids Surfaces* **1989**, *37*, 155.
- (7) Cohen, Stuart, M. A.; Fleer, G. J.; Scheutjens, J. M. H. M. *J. Colloid Interface Sci.* **1984**, *97*, 515, 526.
- (8) Kawaguchi, M.; Chikazawa, M.; Takahashi, A. *Macromolecules* **1989**, *22*, 2195.
- (9) Kawaguchi, M.; Hada, T.; Takahashi, A. *Macromolecules* **1989**, *22*, 4045.
- (10) Van der Beek, G. P.; Cohen, Stuart, M. A.; Fleer, G. J.; Hofman, J. E. *Langmuir* **1989**, *5*, 1180.
- (11) Kawaguchi, M.; Sakakida, K. *Macromolecules*, submitted.
- (12) Berry, G. C. *J. Chem. Phys.* **1966**, *44*, 4550; **1967**, *46*, 1338.
- (13) Furusawa, K.; Yamashita, K.; Konno, K. *J. Colloid Interface Sci.* **1982**, *86*, 35.
- (14) Kawaguchi, M., unpublished data.
- (15) Degussa, Technical Bulletin, No. 11, May, 1980.
- (16) Eisenlauer, J.; Killmann, E. *J. Colloid Interface Sci.* **1980**, *74*, 108.
- (17) Iler, R. *The Chemistry of Silica*; Wiley: New York, 1979.
- (18) Kawaguchi, M.; Hayakawa, K.; Takahashi, A. *Polymer J.* **1980**, *12*, 265.
- (19) Van Damme, H.; Levitz, P.; Bergaya, F.; Alcover, J. F.; Gatin-eau, L.; Fripiat, J. J. *J. Chem. Phys.* **1986**, *85*, 616.
- (20) Kawaguchi, M.; Arai, T., unpublished data.

Registry No. PS, 9003-53-6; silica, 7631-86-9; cyclohexane, 110-82-7; dioxane, 123-91-1.